 doi:10.20944/preprints202208.0043.v1

*Article*

# Upregulation of Cytoglobin in 3D-cultures of Head and Neck Cancer Cells: Role of Hypoxia and Implications for Cisplatin Resistance

**Garret Rochford[1], Rameeza Basar[1], Rose Dhiman[1], Djeren Simitdjioglu[1], Lorna S Thorne[1], Lakis Liloglou[2], Janet M Risk[2] and Nikolas J Hodges[1*]**

[1] School of Biosciences, University of Birmingham, Edgbaston, Birmingham, B15 2TT, UK, [2]Institute of Translational Medicine, University of Liverpool, Liverpool, L69 3BX, UK
* Correspondence: n.hodges@bham.ac.uk

**Abstract:** Cytoglobin has been implicated in a range of pathological conditions including fibrosis and cancer, where cytoglobin expression is linked to hypoxia- and drug-resistance. One disease where there is evidence of a role for cytoglobin is head and neck squamous cell carcinoma, a disease with a poor prognosis and where clinical resistance to platinum-based drugs is common. In the current study, we demonstrate that 3D-culture of head and neck cancer cells (PE/CA-PJ41, Liv-22K) and normal oral keratinocyte cells (NOK-hTERT) results in changes in sensitivity to cisplatin cytotoxicity compared to 2D-cultures. Relative to 2D-cultures, 3D-cultures of PE/CA-PJ41 and NOK-hTERT cells demonstrated increased cisplatin resistance. In contrast, 3D-cultures of Liv-22K cells were more sensitive to cisplatin. Evidence for cisplatin genotoxicity was observed in the form of *GADD45A* activation in PE/CA-PJ41 cells but not the other two cell types investigated. Furthermore, DNA-strand breaks were also detected by the alkaline comet assay in PE/CA-PJ41 cells although levels were not significantly affected by 3D-culture. Cytoglobin expression levels were elevated by 3D-culture in all three cell lines investigated and there were also changes in expression of genes related to cell division (*MKI57, GJB6*), cell adhesion (*CDH1*), stress response (*NFkB, NQO1*) and apoptosis (*Casp3*) but these changes were cell line specific. We also observed consistent transcriptional activation of *HIF1a* in 3D-cultures of all three cell lines, suggestive of hypoxic conditions in spheroids. In support of a direct role of hypoxia in cytoglobin induction, the HIF1a stabiliser cobalt chloride also induced cytoglobin expression in spheroids. Transcriptomic profiling of PE/CA-PJ41 cells over-expressing cytoglobin identified 121 differentially regulated genes, when cells were cultured under hypoxic conditions. Major changes identified included, upregulation of G1/S cell cycle regulation as well as wnt- and RhoGTPase-signalling pathways. In conclusion, 3D-cultures are a useful model to further study the biological function of cytoglobin in head and neck cancer and we provide evidence that further supports a role for cytoglobin in hypoxia-dependent cellular proliferation and phenotypic changes that could contribute to cisplatin resistance *in vivo*.

**Keywords:** cytoglobin; spheroids; hypoxia; HIF1a; head and neck cancer

## 1. Introduction

Cytoglobin (*CYGB)* is a hexacoordinated heme-containing protein with reported functions in cancer progression through mechanisms involving antioxidant defense[1–4] and enhancement of cell survival[5–10]. Evidence has shown that cytoglobin may have a role to play in head and neck cancer progression[2,11], however, uncertainties persist with regard to cytoglobin's function in this process. Head and neck squamous cell carcinomas (HNSCCs) are a group of genetically diverse oral cavity, larynx, and oropharynx cancers, which are difficult to treat, have a poor prognosis and accounted for almost 4,000 deaths in the UK between 2015-2017. Furthermore, there has only been a small (9 %) decline in mortality since the 1970's due to the complex pathophysiology and difficulty in providing

 doi:10.20944/preprints202208.0043.v1

targeted treatment[12]. Presently, treatment includes surgical resection, radiotherapy, and platinum-based chemotherapy, all of which have fallen short of substantially improving the treatment success in this cancer. Major issues include uncertainties about treatment combinations, treatment stratification based on biochemical and genetic markers and chemoresistance.

The tumour microenvironment[13,14] and epigenetic regulation[15,16] are both key factors in determining tumour phenotype and difficulties in modelling these *in vitro* using 2D-cultures has presented a key challenge to improving treatment success. A better understanding cytoglobin expression and function may provide useful insights into the mechanisms underlying cisplatin resistance in HNSCC *in vivo*. As stated above, a major difficulty in examining oncogenesis and treatment approaches in HNSCC and many other cancer types is the availability of an *in vitro* model that recapitulates the tumour microenvironment *in vitro*. Therefore, development of more realistic *in vitro* models is central to the effort to develop greater understanding of tumour physiology and mechanistic therapeutic action. Recently, 3D Multi Cellular Tumour Spheroids (MCTS) have demonstrated a greater ability to mimic the tumour microenvironment and therefore provide a superior model to study phenotypic changes like hypoxic and epigenetic regulation mechanisms that are important in *vivo*[17,18]. One of the consequences of changes in tumour microenvironment is its contribution to the phenomena of drug resistance[19]. Cisplatin remains one of the most important chemotherapeutic currently in use in head and neck cancer treatment however, despite its extensive use in general oncology, therapeutic resistance persists in HNSCC and optimal dosages are still being debated in clinical practice[20–22].

Cytoglobin has been strongly linked to tumour hypoxia and particularly the action of Hypoxia Inducible Factor-1 Alpha (*HIF1A*)[7,11,23–25]. HNSCC 3D tumour models have been previously utilised to study tumour physiology and therapeutic responses[26–29]. With the uncertainties surrounding the specific regulatory mechanisms of cytoglobin in hypoxia, 3D tumour spheroid models provide a good tool to investigate the various aspects of this complex regulation mechanism. Additionally, Epidermal Growth Factor (EGF) is commonly overexpressed in head and neck cancer and as such has been another target for therapeutic action[30]. Cytoglobin has been associated with the action of Fibroblast Growth Factor[31,32]. While these have been therapeutic targets for head and neck cancer it is clear that other factors play a pivotal role in oncogenesis and tumour progression. Cytoglobin has been shown to be active in many of these underlying processes, however its role in the tumour hypoxia and cisplatin sensitivity are yet to be resolved. In the current study, we demonstrate that when compared to 2D-cultures, cytoglobin expression is upregulated in 3D-cultures of two cancer and one normal cell line derived from the upper airway. Furthermore, 3D-culture results in increased resistance to cisplatin in 2 of the 3 cell lines investigated. We also present evidence of multiple cell specific changes in stress-response genes and that upregulation of *CYGB* is related to hypoxia and HIF1a signalling in 3D culture. Finally, microarray data in PE/CA-PJ41 cells provides further insights into the role of cytoglobin under conditions of cellular hypoxia including changes in RhoGTPase- and wnt-signalling pathways, that may contribute to cisplatin resistance *in vivo*.

## 2. Materials and Methods

### *2.1. Mammalian cell culture conditions and maintenance*

The PE/CA-PJ41 (Clone D2, Cat No. 98020207) were purchased from the European Collection of Authentication Cell Cultures (ECACC), Public Health England. NOK-hTERT (normal oral keratinocyte cell) and Liv-22K (cancerous keratinocyte derived from lateral tongue) were a kind gift from Dr Janet Risk at University of Liverpool. PE/CA-PJ41 cells were grown in Roswell Park Memorial Institute media (RPMI-1640) (Sigma, R8758) supplemented with 10 % Foetal Bovine Serum (Sigma, F2442), 2 % L-glutamine 200mM (Sigma, G7513) and 2% Penicillin-Streptomycin (5,000 U/ml) (Gibco, 15070063) in T75 cell culture flasks (Sigma, CLS3276). NOK-hTERT and Liv-22K cells were grown in Keratinocyte Serum-Free Media supplemented with L-glutamine, Epidermal Growth Factor 1-53

 doi:10.20944/preprints202208.0043.v1

(EGF 1-53) and Bovine Pituitary Extract (BPE) (Gibco, 17005042) in T75 cell culture flasks. Cultures were confirmed free of mycoplasma contamination by PCR (EZ-PCR Mycoplasma Test Kit, Geneflow). Cells cultures were incubated at 37 °C in a 5 % $CO_2$ humidified atmosphere. Cells were kept in cell culture media until 80 % confluent and sub-cultured using TrypLE Express (Gibco, 12605028) solution. Dissociation reagent was inactivated in PE/CA-PJ41 cells using FBS supplemented RPMI-1640 while filter sterilised Soybean Trypsin Inhibitor (Gibco, 17075029) in Dulbecco's Phosphate Buffered Saline (Gibco, 14190094) was used to neutralise the catalytic activity of TrypLE Express in NOK-hTERT and Liv-22K cells.

*2.2. 3D cell culture*

PE/CA-PJ41, NOK-hTERT and Liv-22K were grown as detailed above until confluency of 80 % was achieved. Cells were removed from T75 flasks using TrypLE Express dissociation reagent and counted using a haemocytometer. Cells were seeded in 96-well Ultra Low Attachment (ULA) Plates (Greiner, Cat No. 650970) at 2,000 cells per well. Cells were allowed to settle for 10 min at room temperature in a Biosafety Cabinet and were subsequently centrifuged at 150 g for 10 min and incubated 37 °C in a 5 % $CO_2$ humidified atmosphere for 3 days. After 72 h incubation, 50 % of the cell culture media was exchanged with fresh cell culture media and the culture returned to incubation conditions.

*2.3. Cytotoxicity assessment*

Cisplatin (Sigma, P4394) was dissolved in sterilised 0.9 % saline and made to an initial concentration of 2 mM. A working solution of 1.56-400 μM cisplatin was made in supplemented RPMI-1640 for PE/CA-PJ41 cells and EGF, BPE supplemented KSFM for NOK-hTERT and Liv-22K cells. Cytotoxicity assessment of cells in 2D culture was carried out by seeding 10,000 cells into 96-well tissue culture plates and incubated the cells for an initial 24 h prior to addition of cisplatin. Cell culture media was removed and replaced with cisplatin working solution. Cells were incubated for 24 h as described above. CellTitre-Glo® Luminescent Cell Viability Assay (Promega, Cat No G7571) was used to evaluate the cisplatin dose-response[33]. The CellTitre-Glo® Luminescent Cell Viability Assay reagent was incubated in a 1:1 ratio in each well of 96-well plate. Cells were covered and placed on a plate shaker for 10 min. Seventy-five μL of the resulting luminescent lysate solution was transferred to a clear-bottomed white walled 96-well plate. The 96-well plate was covered for 10 min prior to reading auto-luminescence on the Tecan Infinite F200 PRO plate reader. MCTS cultures were grown as described above. MCTS of PE/CA-PJ41, NOK-hTERT and Liv22K were incubated in cisplatin working solution for 24 h after the initial MCTS formation period. CellTitre Glo® 3D Cell Viability Assay (Promega, Cat No G9682) was used to evaluate the cisplatin dose-response of the MCTS cells. The CellTitre Glo® 3D Cell Viability Assay reagent was incubated in a 1:1 ratio in each well of the 96-well ULA plate. Cells were covered and lysed on a plate shaker for 1 h. The resulting luminescent lysate solution (75 μL) was transferred to a clear-bottomed white walled 96-well plate and the luminescence recorded similarly to 2D cell cultures. Both assays for 2D and MCTS cultures were performed in triplicate and contained untreated, vehicle and positive (1 % v/v Triton X-100 in cell culture media) controls.

The MTT assay measures the reductive capacity of mitochondria following cytotoxic insult and is commonly used to measure cellular viability[34]. Cobalt Chloride (Sigma, C8661) was initially dissolved in HyClone™ Cell Culture Grade Water (Fischer, Cat No 10001342) and made up to 25 mM. A working solution in the range of 6.25-800 μM was made in cell culture media. Antimycin A (Sigma, A8674) was initially dissolved in ethanol to a concentration of 1 mg/ml. A working solution in the range of 5-25 μg/ml was made in cell culture media. 5-Azacytadine (Sigma, A2385) was initially dissolved in Dimethyl Sulfoxide (DMSO) (Sigma, D2650) to a concentration of 100 μM. A working solution in the range of 0.156-20 μM was made in cell culture media. PE/CA-PJ41, CG-NOK and Liv-22K cell lines were removed from T75 flasks using the dissociation solution TrypLE Express

Preprints (www.preprints.org) | NOT PEER-REVIEWED | Posted: 2 August 2022 doi:10.20944/preprints202208.0043.v1

as described above. The cells were counted using a haemocytometer and 5,000 cells were seeded in a 96-well plate. The cells were incubated for 24 h prior to drug exposure. Cell culture media was removed and 100 µL of the working solution of either Cobalt Chloride, Antimycin A or 5-azacytadine was added to the cells followed by a 24 h incubation as described above. After the 24 h exposure, the cells were washed with DPBS and incubated with 0.5 mg/mL Thiazolyl Blue Tetrazolium Bromide (MTT) (Sigma, M5655) solution (5 mg/mL stock solution in DPBS, diluted 1:10 in cell culture media) for 3 h at 37 °C in 5 % $CO_2$ humidified atmosphere. The cells were removed and washed twice with DPBS. The formazan salt was dissolved in 100 µL and absorbance read at 595 nm using the Tecan Infinity F200 PRO plate reader.

*2.4. Alkaline Comet Assay*

The comet assay was carried out on both 2D and 3D MCTS cultured PE/CA-PJ41 cells. PE/CA-PJ41 were initially cultured in T75 flasks and chemically dissociated using TrypLE Express as above. Cells were transferred to T25 flasks. 3D MCTS PE/CA-PJ41 were generated as described above. PE/CA-PJ41 cells in T25 and ULA plates (3D MCTS) were exposed to their respective 24 h $IC_{50}$ concentration and incubated for 24 h. Cells were dissociated in TrypLE Express and re-suspended in DPBS to give a final cell concentration of 250,000 cells/ml. Low melting point agarose (0.7 %) (Sigma, A9045) was made in DPBS mixed with cell suspension in a 3:1 ratio (3 parts agarose to 1 part cells). The resulting mixture was used to form 2 mini gels (20 µL each) on a comet slide pre-coated in 1 % normal molecular grade agarose (Sigma, 05066) dissolved in deionised water before being left to dry at 4 °C for 10 min. Comet slides were then incubated in lysis solution (2.5 M NaCl, 0.1 M $Na_2EDTA$, 10 mM Tris base, 1 % sodium N-lauryl sarcosinate, 10 % DMSO and 1 % Triton X-100, adjusted to pH 10.0) overnight at 4 °C and then placed in electrophoresis buffer (75 mM NaOH and 1 mM $Na_2EDTA$, adjusted to pH 12.1) for 20 min. Electrophoresis was carried out at 4 °C, and run at 20 V and 300 mA for 20 min, removed from the tank, covered with neutralisation buffer (0.4 M Tris, adjusted to pH 7.5) for 5 min and fixed in ethanol. Slides were left drying overnight at RT and stained with SYBR gold (Thermo, S11494) (1:1000 in $dH_2O$ at 4°C for 1 h). Cells were visualised on the Axiovert 10 fluorescent microscope (Zeiss, Germany) with a FITC filter installed. Counting and scoring were conducted using Komet IV software (Instem, UK). Fifty cells were counted and scored for each mini gel to give one replicate. Measurement of the percent (%) tail DNA were conducted as a measure of the extent of DNA damage.

*2.5. Gene expression analysis of cytoglobin and hypoxia regulating genes*

2.5.1. Microarray analysis of cytoglobin transfected PE/CA-PJ41 cells in hypoxic conditions

Cytoglobin over-expressing PE/CA-PJ41 cells were transfected with the pCMV6-Neo plasmid containing the human cytoglobin cDNA sequence using Turbofectin 8.0 (Origene, United States) as a transfection agent. Stable clones were selected using the cloning ring method and were expanded in G418 sulfate (Sigma, G418-RO) supplemented RPMI-1640 cell culture media. An additional transfection with an empty plasmid vector was also performed (Mock). PE/CA-PJ41 cells transfected with an empty vector were labelled "Mock" and those with cytoglobin as "CYGB". PE/CA-PJ41 cells expressing CYGB and Mock were labelled with cyanine 5 and 3, respectively, and cRNA (300 ng) was hybridised to an Agilent SurePrint G3 Human Gene Expression 8x 60K v1 Microarray by the Genomic Facility (University of Birmingham) according to the manufacturer's protocol. RNA quality and quality was determined using the 2100 Agilent Bioanalyser.

2.5.2. RNA extraction, cDNA synthesis and qPCR analysis

Cell were washed with DPBS and then removed from the 6-well plates/ 96-well ULA plates (3D MCTS) using TrypLE Express as described above. Cells grown in 2D culture were centrifuged at 120 g for 5 min and re-suspended in fresh DPBS. Cell grown as 3D

Preprints (www.preprints.org) | NOT PEER-REVIEWED | Posted: 2 August 2022 doi:10.20944/preprints202208.0043.v1

MCTS were pelleted at 120 g for 5 min, DPBS removed and pellets snap frozen in liquid nitrogen prior to RNA extraction. Cell grown in 2D culture were pelleted as above, DPBS removed before RNA extraction. RNA extraction was carried out using the RNeasy mini kit (Qiagen, Cat No 74104). The cell pellets were re-suspended and disrupted in 350 µL of RLT buffer. An equal volume of ethanol was added to the lysate followed by its addition to the spin column, which was placed in the collection tube. Samples were spun at 8000 g for 30 sec and flow through discarded. The columns were washed with a series of buffers as per the manufacturer's instructions. The final wash buffer was centrifuged through the columns and was subsequently left to dry for 10 min. The RNA was eluted using 30 µL of non-DEPC treated nuclease free water (Thermo, AM9932). The RNA was quantified and qualified using the NanoDrop™ 8000 Spectrophotemeter with the RNA samples being normalized to 20 ng/µL. cDNA conversion was performed using the High-Capacity cDNA Reverse Transcription Kit (Thermo, 4374966). The normalised RNA samples were mixed with an equal volume of cDNA master mix containing 10 X RT Buffer, 25 X dNTP Mix, 10 X RT Random Primers, MultiScribe™ Reverse Transcriptase, RNase Inhibitor and nuclease free water to a total reaction volume of 20 µL. cDNA was amplified using the Mastercycler® Gradient (Eppendorf, USA) using the following conditions; 25 °C for 10 min, 37 °C for 120 min and 85 °C for 5 min. qPCR was conducted on the cDNA converted templates using Brilliant III Ultra-Fast SYBR® Green QPCR Master Mix (Agilent, 600882). Target and reference genes used for qPCR analysis are displayed in Table S1 Master mixes for each gene of interest and reference gene was prepared using 2X SYBR Green QPCR master mix, upstream primer (500 nM), downstream primer (500 nM), ROX reference dye (30 nM), nuclease-free PCR-grade water and 1 µl of template cDNA (20 ng) to a final volume of 20 µl in each PCR reaction. PCR amplification and melt curve dissociation curves were generated with the AriaMX Real-time PCR System (Agilent, USA) using the following thermal parameters; 95 °C for 3 min, 40 cycles of 95 °C 5 sec and 60 °C 10 sec, followed by a melt dissociation curve. Experiments were performed in triplicate with each reaction technically replicated twice. Template controls were used to confirm the absence of significant autofluorescence. ROX reference dye was included in order to account for small variations in pipetted volume.

### *2.6. Statistical analysis*

CellTitre-Glo® luminescent assay data was normalized to both the positive and vehicle controls with changes in luminescence calculated relative to vehicle control luminescence. The $IC_{50}$ of the cisplatin dose-response was calculated using least squares non-linear regression. Statistical differences between the cisplatin $IC_{50}$ concentrations of the 2D and 3D MCTS of each cell lines was calculated using a Brown-Forsythe and Welch ANOVA test with Dunnett's multiple corrections. The MTT assay data analysed in a similar manner to the CellTitre-Glo® luminescent assay. DNA damage in the comet assay was determined by using the median percent DNA tail in three separate experiments and was statistically analysed using ANOVA and *post-hoc* Student's *t*-tests. Relative gene expression analysis was conducted using the geometric mean Ct value from the actin reference gene. Average Ct values for target genes along with standard deviations were calculated. Gene expression values were normalized in accordance with the Livak and Schmittgen method[35] and displayed as Log(2) transformed values relative to the untreated 2D cell culture. Microarray data was analysed using *t*-tests between mock and CYGB transfected PE/CA-PJ41 cells with False Discovery Rate (FDR) set to 0.05. Gene Set Enrichment Analysis (GSEA) was performed using the online platform Metascape (http://www.metascape.org)[36] on statistically significant differentially abundant genes as determined using Perseus software platform (http://www.perseus-framework.org)[37].

Preprints (www.preprints.org) | NOT PEER-REVIEWED | Posted: 2 August 2022 doi:10.20944/preprints202208.0043.v1

## 3. Results

### *3.1. 3D cell culture alters cellular response to cisplatin and expression of markers of proliferation*

All three cell lines investigated formed condensed, roughly spherical spheroids with a diameter in the region of 200 μm when grown on ultralow attachment plates. Spheroids formed within 48 hours and were maintained for up to 144 hours in culture (Figure 1). To assess the cytotoxic response of cells to cisplatin in 2D- and 3D-culture we quantified cellular ATP levels, a widely used marker of cellular viability[33]. The $IC_{50}$ concentration were determined using non-linear least square regression analysis (Figure S1–S3) and are presented in Figure 2. The Head and neck cancer cell line PE/CA-PJ41 demonstrated moderate resistance to cisplatin exposure ($IC_{50}$ 72.9 μM), which statistically significantly increased to 110.3 μM in 3D-culture (Figure 2). The primary normal cell line, NOK-hTERT was more sensitive to cisplatin in 2D culture ($IC_{50}$ 14.79 μM) but also showed an increase in resistance in 3D-culture ($IC_{50}$ 65.6 μM) (Figure 2). In contrast, the primary cancer cell Liv-22K demonstrated a different response profile to cisplatin to that of PE/CA-PJ41 and NOK-hTERT cells with an $IC_{50}$ of 93.2 μM, comparable to PE/CA-PJ41 in 2D culture but became significantly more sensitive to cisplatin when cultured as spheroids ($IC_{50}$ 42.2 μM) (Figure 2).

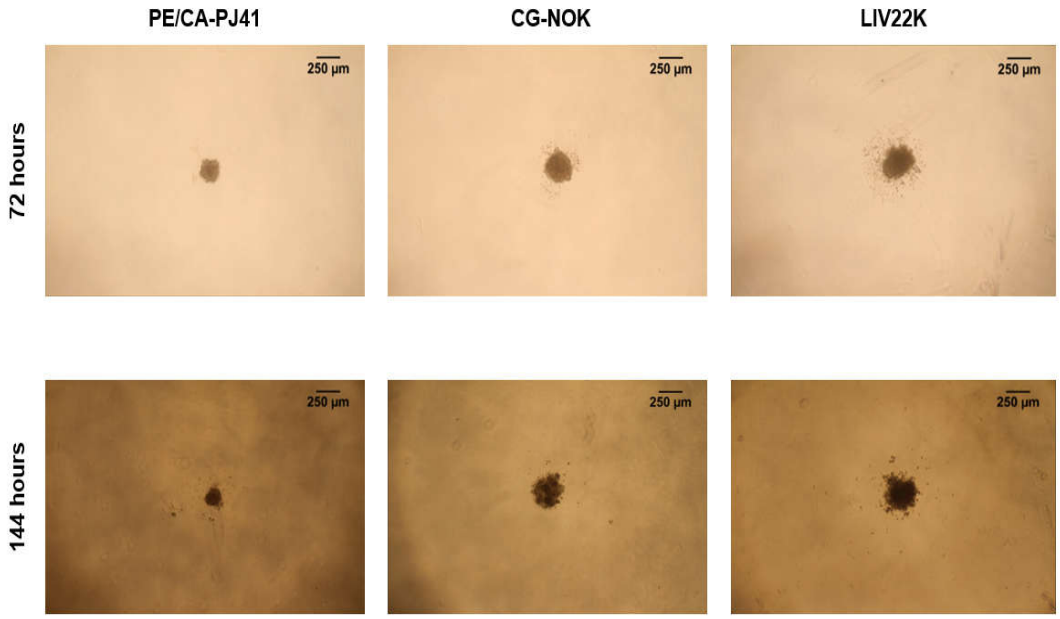


**Figure 1.** Representative images of 3D MCTS of PE/CAPJ41, NOK-hTERT and Liv-22K cells 72 and 144 h after seeding in 96-well ULA plates.

Preprints (www.preprints.org) | NOT PEER-REVIEWED | Posted: 2 August 2022 doi:10.20944/preprints202208.0043.v1

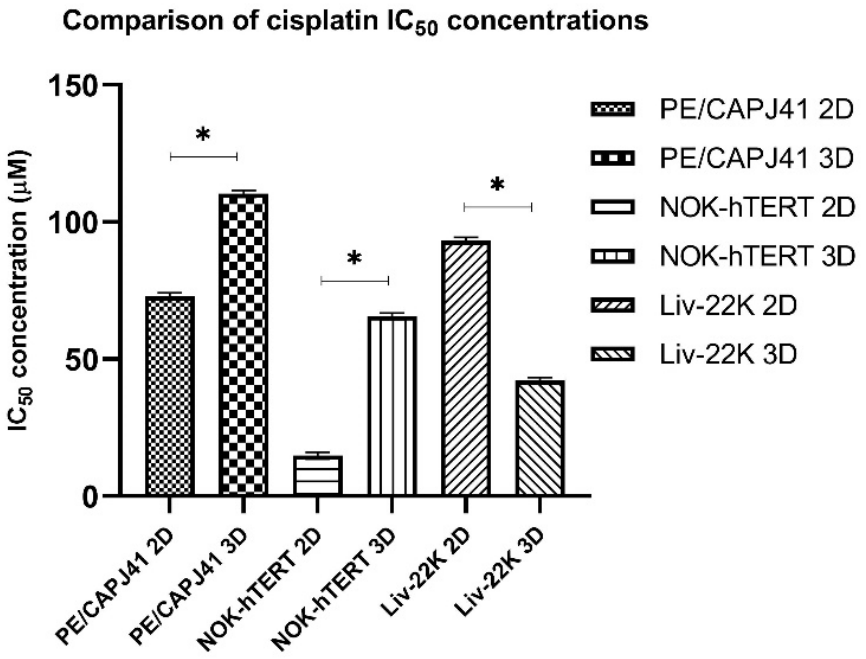


**Figure 2.** Cisplatin $IC_{50}$ concentrations measured using the CellTitre Glo luminescent assay in PE/CAPJ41, NOK-hTERT and Liv-22K cell lines both in 2D and in 3D MCTS culture. Statistical comparison calculated using Brown-Forsythe and Welch ANOVA test with Dunnetts multiple corrections. $p < 0.05$.

The cellular proliferation markers *MKI67*, *GJB6* and *CDH1* were quantified using qPCR gene expression analysis (Figure 3). Compared to untreated 2D-cultures, expression of *MKI67* was downregulated in PE/CA-PJ41 in response to both cisplatin and 3D-culture. Treatment of 3D-cultures with cisplatin had no further effect on expression. In contrast, in primary cancer cells (Liv-22K) *MKI67* expression was not affected by cisplatin treatment in 2D-cultures but was strongly induced by 3D-culture an effect that was further enhanced by treatment with cisplatin. Finally, in primary normal cells (NOK-hTERT) *MKI67* expression was also strongly induced by cisplatin and 3D-culture. Gap junction B6 (*GJB6*) was upregulated by both cisplatin and 3D culture in PE/CA-PJ41, in contrast, in Liv-22K and NOK-hTERT cell lines it was strongly induced by cisplatin but downregulated in response to 3D-culture. Finally, E-cadherin (*CDH1*) gene expression was upregulated in 3D-cultures of PE/CA-PJ41, an effect that was further increased by treatment with cisplatin. In contrast, in both Liv-22K and NOK-hTERT cell lines E-cadherin expression was upregulated in response to cisplatin treatment in both 2D and 3D-cell cultures, but 3D-culture alone had no effect on expression levels.

Preprints (www.preprints.org) | NOT PEER-REVIEWED | Posted: 2 August 2022 doi:10.20944/preprints202208.0043.v1

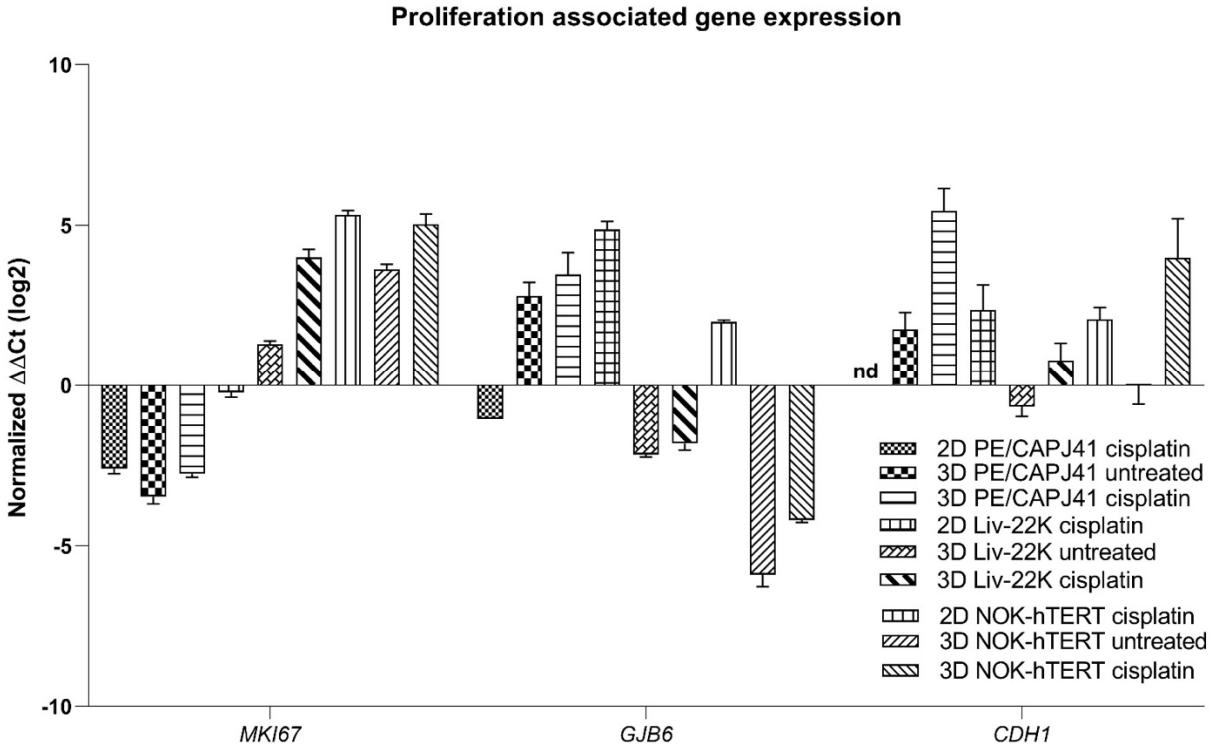


**Figure 3.** Represents the relative expression of proliferation associated genes to the 2D untreated cultures of the indicated cell lines. Expression of genes measured in cisplatin treated ($IC_{50}$ concentration), 3D MCTS untreated and 3D MCTS cisplatin treated ($IC_{50}$ concentration) PE/CAPJ41, NOK-hTERT and Liv22K cells. nd=not detected. N=3.

*3.2. Cisplatin genotoxicity and transcriptional response*

The alkaline comet assay (Figure 4) demonstrated that cisplatin treatment in both 2D- and 3D-cultures of PE/CA-PJ41 cells induced significant DNA-strand breaks in this cell line. However, there was no significant difference in levels of DNA-strand breaks induced by cisplatin in 2D- and 3D-cultures. Interestingly, there was a small but statistically significant increase in background levels of DNA-strand breaks in 3D-cultures compared to 2D-cultures. qPCR analysis (Figure 5) of genotoxicity and transcriptional response quantified changes in expression of *GADD45A*, a transcriptional marker of DNA-strand breaks, *Casp3* the executioner caspase involved in cell death by apoptosis and *NFκB*, a marker of early-stage inflammation. Consistent with DNA-strand breaks, *GADD45A* was strongly induced by cisplatin in both 2D- and 3D-cultures of PE/CA-PJ41 cells but was down regulated under control 3D culture conditions. Interestingly, in contrast, *GADD45A* showed negative regulation in NOK-hTERT and Liv22K cells. *Casp3* demonstrated upregulation in 3D-cultures of PE/CA-PJ41, which was further enhanced by treatment with cisplatin. In Liv22K cells, *Casp3* was upregulated by 3D-culture but not affected by treatment with cisplatin and finally was downregulated in all cultures of NOK-hTERT. *NFκB* demonstrated strong induction in PE/CA-PJ41 cells in response to cisplatin and 3D culture (16-fold induction) but interestingly only minor increases were observed in response to cisplatin or culture conditions in either NOK-hTERT or Liv22K cells.

Preprints (www.preprints.org) | NOT PEER-REVIEWED | Posted: 2 August 2022 doi:10.20944/preprints202208.0043.v1

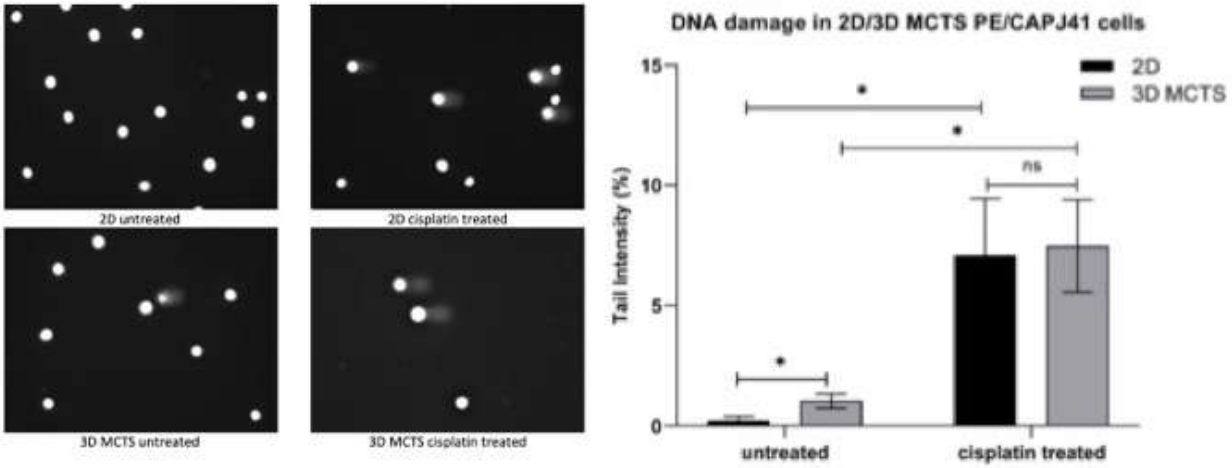


**Figure 4.** Comet assay illustrating DNA damage (comet "tail") in PE/CAPJ41 cells after exposure to cisplatin ($IC_{50}$ concentration) in 2D and 3D MCTS culture. Statistical comparison using Welch's *t*-test, $p < 0.05$. N=3.

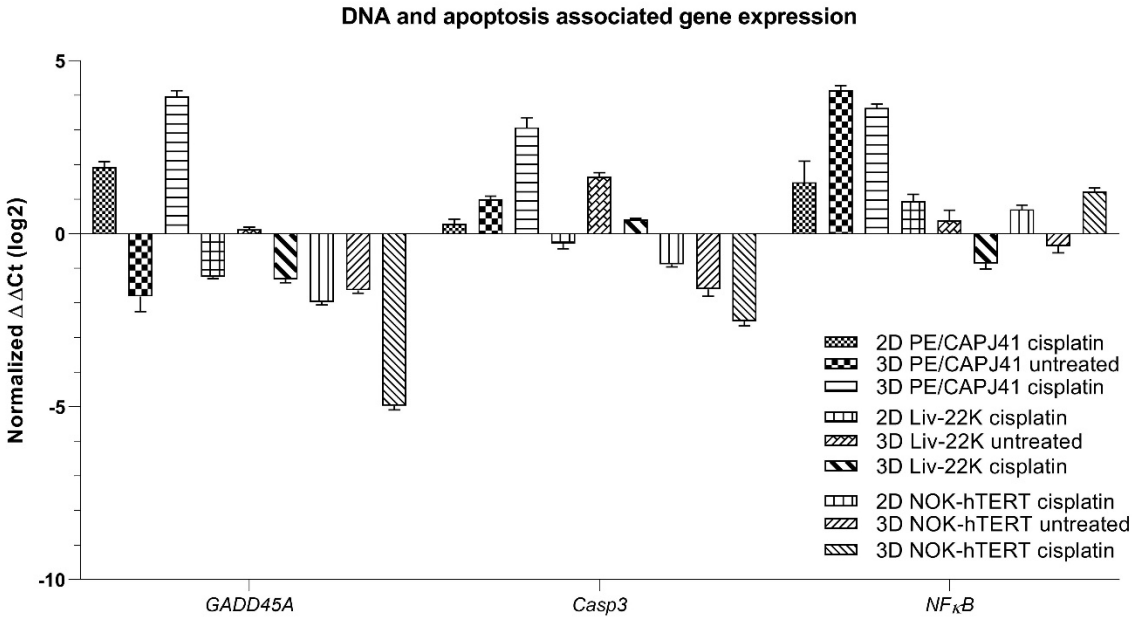


**Figure 5.** Represents the relative expression of DNA damage and cytotoxicity associated genes to the 2D untreated cultures of the indicated cell lines. Expression of genes measured in cisplatin treated ($IC_{50}$ concentration), 3D MCTS untreated and 3D MCTS cisplatin treated (IC50 concentration) PE/CAPJ41, NOK-hTERT and Liv22K cells. N=3.

3.3.3. D culture regulates expression of cytoglobin and other stress response genes

Expression of cytoglobin was measured using both flow cytometry (immunodetection, Figure 6 A–C) and qPCR analysis (Figure 6 D). Immunofluorescence demonstrated no significant change in cytoglobin protein levels after cisplatin treatment ($IC_{50}$ concentration) in 2D-cultures of PE/CA-PJ41 and NOK-hTERT but a significant increase in Liv22K cells after treatment with cisplatin. Gene expression analysis of cytoglobin (*CYGB*) demonstrated only minor or no induction after treatment with cisplatin in 2D cell cultures. However, in 3D culture, induction was observed in PE/CA-PJ41 (32-fold), Liv22K (2-fold) and NOK-hTERT (8-fold) (Figure 6D). In addition, levels of *CYGB* remained elevated or where enhanced further following treatment with cisplatin (Figure 6D). Interestingly, treatment of PE/CA-PJ41 and Liv22K cells with 5-azacytadine also resulted in an increase

Preprints (www.preprints.org) | NOT PEER-REVIEWED | Posted: 2 August 2022 doi:10.20944/preprints202208.0043.v1

in *CYGB* expression which was enhanced in 3D-culture. In contrast, *CYGB* expression was downregulated in NOK-hTERT cells following treatment with 5-azacytadine. Together, these results suggest a possible role for epigenetic regulation of *CYGB* in HNSCC cell cultures but that this appears to be cell specific. To investigate a possible role of hypoxia in 3D-cultures, *HIF1A* expression was quantified. *HIF1A* expression was upregulated in 3D untreated (8-fold), and cisplatin treated PE/CA-PJ41 cells (8-fold) but interestingly, in contrast was downregulated in both 3D untreated and cisplatin treated Liv22K and NOK-hTERT cells suggesting that different extents of hypoxia exist in spheroids derived from different cell lines. Furthermore, treatment with 5-azacytadine resulted in induction of *HIF1A* in all cell lines. The quinone reductase *NQO1* has a major role in cellular redox control and was also quantified. Expression of *NQO1* followed the same upregulation in PE/CA-PJ41 as *CYGB* with induction of approximately 4-fold under both culture conditions. However, *NQO1* was downregulated following 3D-culture and cisplatin treatment in the other 2 cell lines investigated. Finally, to further investigate potential epigenetic regulation, the methyl transferase *DNMT1* was also quantified by qPCR. Expression of *DNMT1* was generally downregulated over most of the cell lines and experimental conditions investigated. PE/CA-PJ41 cells were relatively insensitive to the methyl transferase inhibitor, however 5-azacytadine induced substantial downregulation of *DNMT1* in both the 3D Liv22K and NOK-hTERT cells.

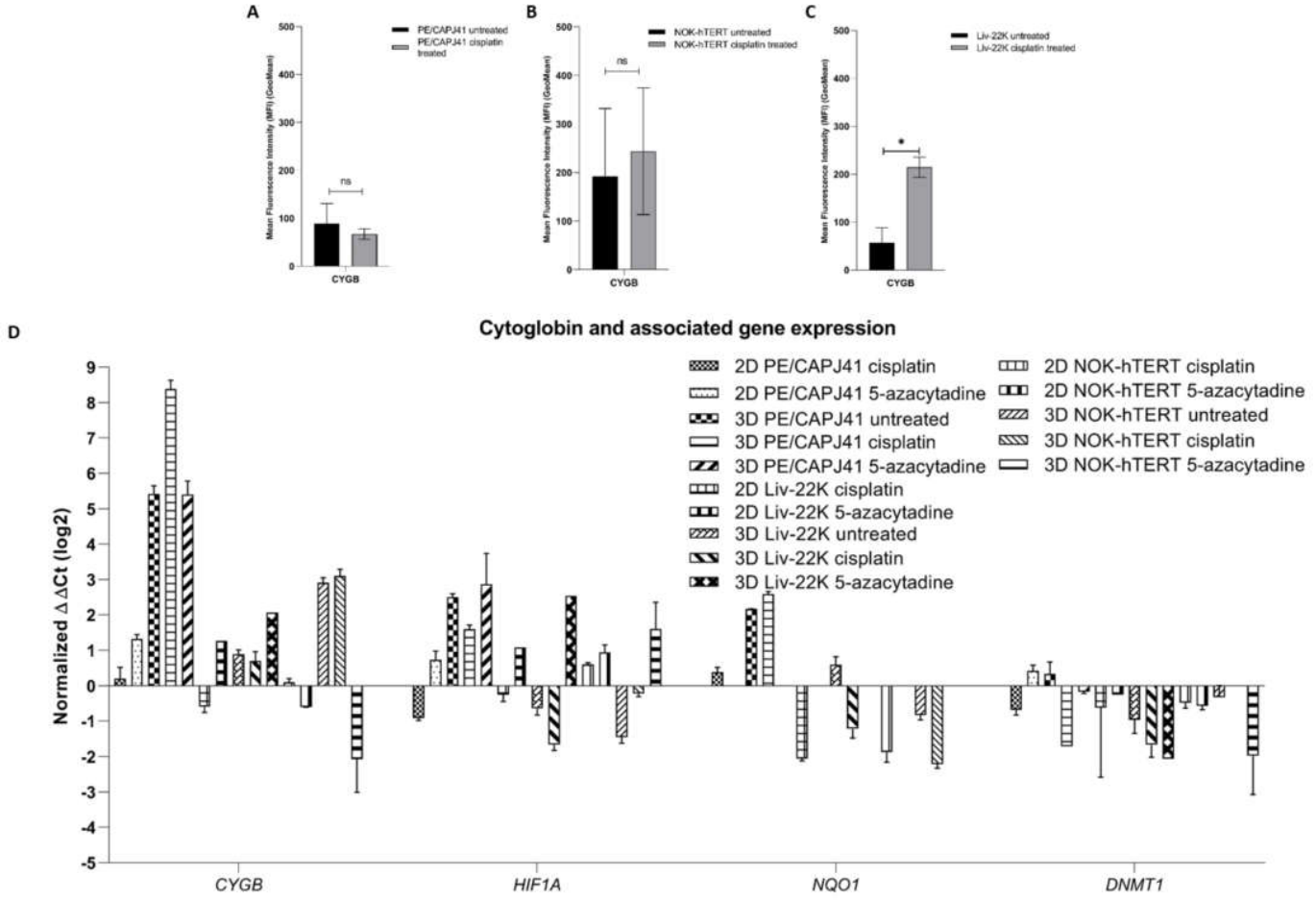


**Figure 6. A)** represents the induction of cytoglobin in PE/CAPJ41 cells untreated and after cisplatin treatment ($IC_{50}$ concentration) for 24 h. **B)** represents induction of cytoglobin in NOK-hTERT cells untreated and after cisplatin treatment ($IC_{50}$ concentration) for 24 h. **C)** represents the induction of cytoglobin in Liv-22K cells untreated and after cisplatin treatment ($IC_{50}$ concentration) for 24 h. **D)** represents the relative expression of cytoglobin associated genes to the 2D untreated cultures of the indicated cell lines. Expression of genes (*CYGB*, *HIF1A*, *NQO1* and *DNMT1*) measured in cisplatin treated 2D/3D ($IC_{50}$ concentration), 3D untreated and 2D/3D 5-azacytadine treated (100 nM)

 doi:10.20944/preprints202208.0043.v1

PE/CAPJ41, NOK-hTERT and Liv22K cells. * Indicates $p < 0.05$ based on Welsh's *t*-test comparing untreated cells with cisplatin treated cells. ns = no significant difference. N=3.

### *3.4. Transcriptomic profiling of cytoglobin expressing PE/CA-PJ41 cells in hypoxic conditions*

Because expression of *CYGB* and *HIF1A* was strongly upregulated in 3D-cultures of PE/CA-PJ41 cells (Figure 6), we wanted to further investigate transcriptional changes regulated by *CYGB* by hypoxia in this cell line. Therefore, a cDNA microarray experiment was undertaken to identify differentially expressed genes under conditions of cellular hypoxia in PECA/PJ41 cells genetically engineered to overexpress *CYGB* described previously[38]. Control and *CYGB* expressing PE/CA-PJ41 were exposed to hypoxia (1 % $O_2$, 12 hours) and gene expression analysed using an Agilent SurePrint G3 Human Gene Expression 8x Microarray. Statistical analysis using Principal Component Analysis (PCA) (Figure S4A), volcano plot (Figure S4B) and Hierarchical Clustering (Figure S5) identified 121 statistically significantly differentially expressed genes in *CYGB* expressing cells compared to non-expressing cells. Of these, 54 were significantly differentially upregulated in *CYGB* expressing cells (Figure S4B) and 67 genes down regulated (Figure S4B). GSEA analysis was performed on the 54 differentially upregulated gene in the *CYGB* expressing cells. (Table S2) GSEA analysis (Figure 7) identified significant enrichment of the Reactome gene set for Cyclin E associated events during G1/S transition (R-HAS-69202). Gene ontology molecular functions demonstrated significant enrichment of Rho GTPase binding (GO:0017048). Gene ontology biological processes demonstrated significant enrichment of the following processes: Rho protein signal transduction (GO:0007266), Wnt signalling pathway (GO:0016055) and cell division (GO:0051301). GSEA also identified significant enrichment of the KEGG pathway Axon guidance (hsa04360). Additionally, several of the enriched genes are present in more than one category. Differentially downregulated genes are shown in Table S3. To further investigate the role of hypoxia and redox stress in gene expression response of *CYGB*, *HIF1A* and *DNMT1* in PE/CA-PJ41, Liv22K and NOK-hTERT cells were examined after exposure to the hypoxia inducer cobalt chloride, the redox inducers hydrogen peroxide and antimycin A and the demethylating nucleoside analogue 5-azacytadine. After initial cytotoxicity assessment to establish $IC_{50}$ values (Figure S6) changes in gene expression where quantified by qPCR (Figure 8). Cobalt chloride exposure resulted in the upregulation of *HIF1A* expression in all cell lines however; Liv22K demonstrated the highest upregulation. *CYGB* and *DNMT1* were upregulated following cobalt chloride treatment in PE/CA-PJ41 and Liv22K but slightly downregulated in NOK-hTERT cells. In contrast, exposure to hydrogen peroxide (1 μM) or antimycin A ($IC_{50}$ concentration) results in only minor changes in the levels of expression of *CYGB*, *HIF1A* and *DNMT1* in PE/CA-PJ41, Liv22K and NOK-hTERT cells.

Preprints (www.preprints.org) | NOT PEER-REVIEWED | Posted: 2 August 2022 doi:10.20944/preprints202208.0043.v1

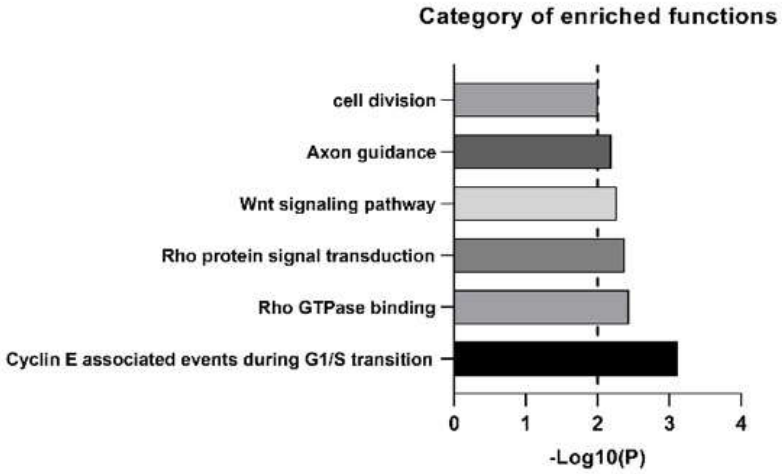


| Category | Term | Category description | LogP | InTerm_In List | Symbols and gene name |
|---|---|---|---|---|---|
| Reactome Gene Sets | R-HSA-69202 | Cyclin E associated events during G1/S transition | -3.11 | 3/83 | **PSMB9 (proteasome (prosome, macropain) subunit, beta type, 9)**<br>PTK6 (PTK6 protein tyrosine kinase 6)<br>**WEE1 (WEE1 homolog (S. pombe)**<br>**NRP1 (neuropilin 1)** |
| GO Molecular Functions | GO:0017048 | Rho GTPase binding | -2.43 | 3/143 | DIAPH2 (diaphanous homolog 2 (Drosophila))<br>EPS8L2 (EPS8-like 2)<br>**PARD6B (par-6 partitioning defective 6 homolog beta (C. elegans))** |
| GO Biological Processes | GO:0007266 | Rho protein signal transduction | -2.38 | 3/150 | ARHGAP5 (Rho GTPase activating protein 5)<br>**NRP1 (neuropilin 1)**<br>EPS8L2 (EPS8-like 2) |
| GO Biological Processes | GO:0016055 | Wnt signaling pathway | -2.27 | 5/525 | FOXL1 (forkhead box L1)<br>**PSMB9 (proteasome (prosome, macropain) subunit, beta type, 9)**<br>SULF2 (sulfatase 2)<br>NDRG2 (NDRG family member 2)<br>CTHRC1 (collagen triple helix repeat containing 1) |
| KEGG Pathway | hsa04360 | Axon guidance | -2.19 | 3/175 | **NRP1 (neuropilin 1)**<br>**PARD6B (par-6 partitioning defective 6 homolog beta (C. elegans))**<br>SSH2 (slingshot homolog 2 (Drosophila)) |
| GO Biological Processes | GO:0051301 | cell division | -2.00 | 5/609 | CALM3 (calmodulin 3 (phosphorylase kinase, delta))<br>**WEE1 (WEE1 homolog (S. pombe))**<br>MIS18BP1 (MIS18 binding protein 1)<br>**PARD6B (par-6 partitioning defective 6 homolog beta (C. elegans))**<br>LRRCC1 (leucine rich repeat and coiled-coil domain containing 1) |

**Figure 7.** Significantly enriched gene ontology categories after GSEA using Metascape. Inset table displays gene component of each enrichment category. **Bold** indicates genes that enrich more than one category.

Preprints (www.preprints.org) | NOT PEER-REVIEWED | Posted: 2 August 2022 doi:10.20944/preprints202208.0043.v1

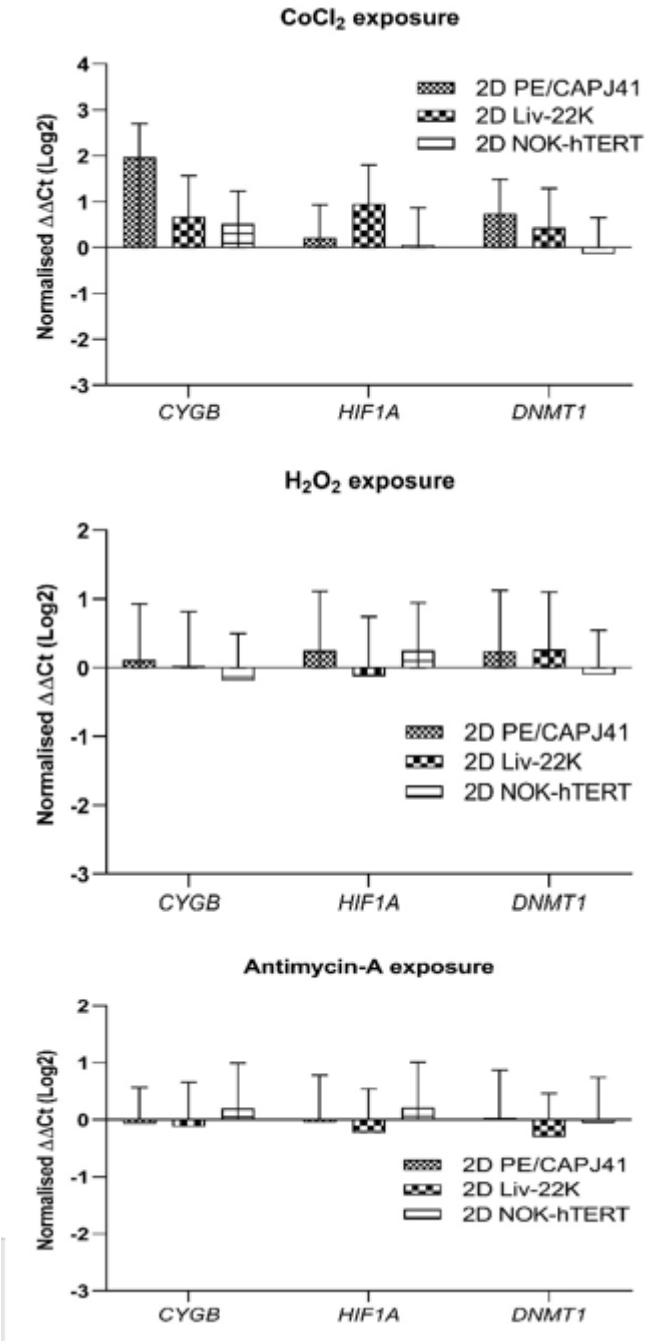


**Figure 8.** Gene expression analysis of *CYGB*, *HIF1A* and *DNMT1* in response to; cobalt chloride ($IC_{50}$ concentration), hydrogen peroxide (1 μM) and antimycin A ($IC_{50}$ concentration). N=3.

## 4. Discussion

The ability to culture cancer cells as 3D-spheroids has provided a new model to study therapeutic response to chemotherapeutic agents including cisplatin[13,19,28]. Cytoglobin has previously been shown to be involved in cancer progression[39] along with potential roles in oxygen sensing[40], detoxification of ROS[3,41,42] as well as protection against hypoxia[6,11,43]. The enhanced ECM environment and generation of a hypoxic core in the centre of cancer cell line spheroids provides an opportunity to evaluate the contribution of cytoglobin and hypoxia to the cisplatin therapeutic response in a more physiologically relevant *in vitro* model. Generation of spheroid from PE/CA-PJ41 cells has previously been demonstrated[44] and in this study they were used as a "*reference*" immortalised HNSCC cancer cell line. Additionally, the primary normal oral Keratinocyte NOK-hTERT and cancerous Liv-22K

Preprints (www.preprints.org) | NOT PEER-REVIEWED | Posted: 2 August 2022 doi:10.20944/preprints202208.0043.v1

provided a basis for comparing primary cells with an established cell line. Cell viability assays demonstrated changes in cisplatin $IC_{50}$ values when cells were grown as 3D spheroids. Typically making cell lines more resistant to cisplatin. In agreement with our findings, previous studies have demonstrated similar increases in resistance profiles to various drugs in tumour spheroid, which are believed to better model *in vivo* solid tumours[19,45]. In our study, the PE/CA-PJ41 and Liv22K cells showed a greater resistance to cisplatin than the primary normal NOK-hTERT cells.

A major mode of action of cisplatin is through the formation of genotoxic DNA-cross-links and DNA-strand breaks were confirmed directly in both 2D- and 3D-PECAPJ/41 cultures using the alkaline comet assay. *CYGB* has been previous linked to p53 dependent apoptosis[46,47] and protection from cisplatin-induced cytotoxicity through regulation of the mitochondrial redox sensitive cardiolipin family of lipids[38]. Intriguingly, there is evidence that haemoglobin and myoglobin can physically interact with cisplatin[48]. Although it is not known if cisplatin is able to interact with cytoglobin this could be represent another direct mechanism of cellular protection from cisplatin. The cellular response to genotoxic stress involves upregulation of *GADD45A* expression and loss of *CYGB* expression has been linked to decreased expression of *GADD45A* and other p53-dependent pro-apoptosis factors[49]. Interestingly, in the current study, in primary cell lines we observed down regulation of *GADD45A* in response to both cisplatin treatment and 3D cell culture suggesting that a p53 independent damage response mechanism may be occurring in these cell lines. Caspase 3 (*Casp3*) is a key effector gene in the intrinsic apoptosis pathway and is upregulated in PE/CA-PJ41, and to a lesser extent in the primary cancer cells Liv22K. In contrast, the primary normal cell line NOK-hTERT demonstrated downregulation of caspase 3 and *GADD45A,* which are strongly associated with p53-dependent action[50]. NOK-hTERT cells overexpress telomerase reverse transcriptase and in doing so function as an immortalised primary derived model of oral keratinocytes[51]. Over expression of hTERT is known to suppress p53-mediated apoptosis[52], which may explain the disparity between the PE/CA-PJ41 and Liv22K cells with the NOK-hTERT cell. Early stage inflammation measured through *NFκB* expression presented a similar pattern of expression to that of *Casp3* expression. Upregulation of *NFκB* has been associated with cytoglobin mediated cell survival against oxidative stress[10]. Surprisingly, the same level of upregulation is not observed in the Liv22K and NOK-hTERT suggesting that the formation of spheroids and exposure to cisplatin in 3D has a limited ability to initiate the apoptotic response through *GADD45A*, *Casp3* and *NFκB* and that regulation of these pathways appears to be cell line specific. The alkaline comet assay demonstrated that growth of cell as 3D-cutures induced a small but significant increase in background levels of DNA damage. The induction of hypoxia in the 3D-cultures has been shown to initiate greater DNA damage when transitioning from 20 % to 1 % $O_2$ tension[53]. However, cisplatin treatment showed no significant difference between 2D- and 3D-cultures suggesting that the induction of hypoxia may be a greater driving force behind the DNA damage than cisplatin exposure in this model. Additionally, from the gene expression panel the increasing induction of *GADD45A*, *Casp3* and *NFκB* in 2D towards 3D cisplatin treatment demonstrates the potential role of p53-dependent PI3K/AKT-caspase3 pathways in cytotoxicity[54].

Immunofluorescence analysis of cytoglobin protein levels determined that no significant changes occurred between untreated, and cisplatin treated PE/CA-PJ41 and NOK-hTERT. Analysis by qPCR showed transcriptional activation of *CYGB* in 3D-cultures of all three cell lines investigated. However, this was not markedly affected further by treatment with cisplatin except in PE/CA-PJ41 cells. Evidence of hypoxia in 3D-cultures was assessed by quantification of expression of *HIF1A*. Previously, studies have shown a link between induction of hypoxia and the expression of cytoglobin[11,23,24]. In this study, *HIF1A* expression was upregulated in 3D untreated (8-fold), and cisplatin treated PE/CA-PJ41 cells (8-fold) but interestingly, in contrast was downregulated in both 3D untreated and cisplatin treated Liv22K and NOK-hTERT cells suggesting that different extents of hypoxia exist in spheroids from different cell lines or that the response is cell line specific. The observation that cobalt chloride, a known activator of HIF1a induces cytoglobin

Preprints (www.preprints.org) | NOT PEER-REVIEWED | Posted: 2 August 2022 doi:10.20944/preprints202208.0043.v1

expression, further supports a direct role of hypoxia and HIF1a in the regulation of cytoglobin in spheroid cultures. Interestingly, while *HIF1A* expression is upregulated in 5-azacytadine treated 3D cultures, the activity of the demethylating enzyme *DNMT1* is downregulated in all 5-azacytadine treated 3D spheroids indicating that methylation may play role in the regulation of *HIF1A* in 3D spheroids while *HIF1A* appears to be exclusively associated with *CYGB* expression in PE/CA-PJ41 cells. Furthermore, induction of hypoxia-inducible factor is known to have a role in epigenetic regulation of different cellular process[55]. Cytoglobin expression has previously been shown to be downregulated by promotor hypermethylation[56] and upregulated by tumour hypoxia[11]. Our data suggests that hypermethylation of *HIF1A* and *CYGB* in 3D-culture may be a possible regulator of *CYGB* expression in PE/CA-PJ41, but this would need to be confirmed directly (e.g., by pyrosequencing). There is evidence to suggest that hypoxia is not only a driver of epigenetic regulation but it itself is also effected by methylation status[57]. NAD(P)H quinone oxidoreductase 1 (*NQO1*) is induced in many cellular stress conditions including oxidative stress[58]. *NQO1* is considered a marker of cancer progression and has demonstrated an ability to upregulated anti-apoptosis factors such as *XIAP*[59] and inhibit the proteasome-mediated degradation of *HIF1A*[60], thereby potentiating the hypoxia response. Interestingly, PE/CA-PJ41 cells only demonstrate upregulation of *NQO1* in 3D untreated and cisplatin treated cells, possibly as a response to either hypoxia through *HIF1A* and *CYGB* regulation although further experiments are required to confirm this.

The expression of E-cadherin (*CDH1*) is often associated with the formation of 3D spheroid cultures and its absence usually results in lack of spheroid formation or loose aggregates[61]. Our study demonstrates increases in *CDH1* expression along with decreases in *MKI67* during spheroid formation which has been previously demonstrated in the successful formation of PE/CA-PJ41 spheroids[62]. Interestingly, the production of 3D spheroids of Liv22K and NOK-hTERT cells occurs in the absence of strong *CDH1* expression and is accompanied by increases in the proliferation marker *MKI67*, which is absent in PE/CA-PJ41 cells. The primary Liv22K and NOK-hTERT express EGFR and are supplemented with EGF in culture. EGF signalling has been shown to be involved in the formation of spheroids in head and neck cancer[28,29]. In addition to *MKI67* and *CDH1*, the gap junction gene *GJB6*, often upregulated with detoxification processes,[60] is also upregulated in PE/CA-PJ41 spheroids but only cisplatin treated Liv22K and NOK-hTERT 2D cells, indicating that the *GJB6* may contribute to the increased resistance to cisplatin in PE/CA-PJ41 spheroids[63]. The GSEA-analysis conducted on the microarray dataset determined that *CYGB* expression in hypoxia-enriched pathways was associated with regulation of cell division and other related process. Enrichment of the Rho- and Wnt-signalling pathway has been shown to be closely associated with cells division and motility[64,65], however, Wnt-signalling has more recently become recognised as a mechanism that contributes to oncogenesis[66]. Indeed, the combination of hypoxia and Wnt signalling has been associated with the progression of lung cancer[67] and hepatocellular carcinoma[68]. Overall, cytoglobin expression in cells appears to result in an increased proclivity to for cell cycle progression, changes in mobility and division under conditions of hypoxia that contribute to a malignant phenotype and drug resistance *in* vivo. Although more research is required, this could potentially be through use of hypoxia related activation of Rho- and Wnt-signalling pathways.

## 5. Conclusions

In summary, this study investigated the regulation of cytoglobin in normal and cancer-derived primary head and neck cells along with the cell line model PE/CA-PJ41. All cell lines demonstrated the ability to form 3D-cultures and *CYGB*-expression was elevated in all 3D-cultures examined compared to 2D-cultures of the same cell line. In the PE/CA-PJ41 cell line there was a correlation between hypoxia induction and cytoglobin expression, which was also accompanied by an increase in cisplatin resistance. Furthermore, microarray analysis also revealed that expression of cytoglobin might aid in hypoxia

 doi:10.20944/preprints202208.0043.v1

dependent cellular proliferation and phenotypic changes that could contribute to cisplatin resistance *in vivo*.

**Supplementary Materials:** Supplementary Materials and Methods, Supplementary Figure S1: Concentration-response curve of PE/CAPJ41 in response to cisplatin treatment; Supplementary Figure S2: Concentration-response curve of Liv-22K in response to cisplatin treatment; Supplementary Figure S3: Concentration-response curve of NOK-hTERT in response to cisplatin treatment; Supplementary Figure S4: Principal component and volcano plot analysis of microarray data: Figure S5: Hierarchical clustering analysis of microarray data; Figure S6: Concentration response curves for cobalt chloride, antimycin A and 5-azacytidine; Table S1: Sequences of primers used for qPCR; Table S2: List of statistically significant differentially expressed genes upregulated in *CYGB* expressing PE/CA-PJ41 cells, Table S3: List of statistically significant differentially expressed genes downregulated in *CYGB* expressing PE/CA-PJ41 cells

**Author Contributions:** GR: RB, RD, and DS undertook the experiments except for the microarray experiment that was undertaken by LST. The study was planned by NJH, and the data was analysed and interpreted by NJH with help from GR, LL and JMR. Cell lines used in the study were kindly provided by LL and JMR. All authors read and approved the manuscript

**Funding:** The authors would like to thank The Humane Research Trust (THRT), registered charity number 267779 for funding that has made this research possible.

**Conflicts of interest:** The authors declare no conflict of interest

**Data availability statement:** All data is available from the corresponding author on request

## References

1. Thi Thanh Hai, N.; Thuy, L. T. T.; Shiota, A.; Kadono, C.; Daikoku, A.; Hoang, D. V.; Dat, N. Q.; Sato-Matsubara, M.; Yoshizato, K.; Kawada, N. Selective Overexpression of Cytoglobin in Stellate Cells Attenuates Thioacetamide-Induced Liver Fibrosis in Mice. *Sci. Rep.* **2018**, *8* (1), 17860.
2. McRonald, F. E.; Risk, J. M.; Hodges, N. J. Protection from Intracellular Oxidative Stress by Cytoglobin in Normal and Cancerous Oesophageal Cells. *PLoS One* **2012**, *7* (2).
3. Fordel, E.; Thijs, L.; Martinet, W.; Lenjou, M.; Laufs, T.; Van Bockstaele, D.; Moens, L.; Dewilde, S. Neuroglobin and Cytoglobin Overexpression Protects Human SH-SY5Y Neuroblastoma Cells against Oxidative Stress-Induced Cell Death. *Neurosci. Lett.* **2006**, *410* (2), 146–151.
4. Xu, R.; Harrison, P. M.; Chen, M.; Li, L.; Tsui, T.; Fung, P. C. W.; Cheung, P.; Wang, G.; Li, H.; Diao, Y.; et al. Cytoglobin Overexpression Protects against Damage-Induced Fibrosis. *Mol. Ther.* **2006**, *13* (6), 1093–1100.
5. Fujita, Y.; Koinuma, S.; De Velasco, M. A.; Bolz, J.; Togashi, Y.; Terashima, M.; Hayashi, H.; Matsuo, T.; Nishio, K. Melanoma Transition Is Frequently Accompanied by a Loss of Cytoglobin Expression in Melanocytes: A Novel Expression Site of Cytoglobin. *PLoS One* **2014**, *9* (4), e94772.
6. Nishi, H.; Inagi, R.; Kawada, N.; Yoshizato, K.; Mimura, I.; Fujita, T.; Nangaku, M. Cytoglobin, a Novel Member of the Globin Family, Protects Kidney Fibroblasts against Oxidative Stress under Ischemic Conditions. *Am. J. Pathol.* **2011**, *178* (1), 128–139.
7. Jusman, S. W. A.; Iswanti, F. C.; Suyatna, F. D.; Ferdinal, F.; Wanandi, S. I.; Sadikin, M. Cytoglobin Expression in Oxidative Stressed Liver during Systemic Chronic Normobaric Hypoxia and Relation with HIF-1α. *Med. J. Indones.* **2014**, *23* (3), 133.
8. Latina, A.; Viticchiè, G.; Lena, A. M.; Piro, M. C.; Annicchiarico-Petruzzelli, M.; Melino, G.; Candi, E. ΔNp63 Targets Cytoglobin to Inhibit Oxidative Stress-Induced Apoptosis in Keratinocytes and Lung Cancer. *Oncogene* **2016**, *35* (12), 1493–1503.
9. Mimura, I.; Nangaku, M.; Nishi, H.; Inagi, R.; Tanaka, T.; Fujita, T. Cytoglobin, a Novel Globin, Plays an Antifibrotic Role in the Kidney. *Am. J. Physiol. Physiol.* **2010**, *299* (5), F1120–F1133.
10. Zhang, S.; Li, X.; Jourd'heuil, F. L.; Qu, S.; Devejian, N.; Bennett, E.; Jourd'heuil, D.; Cai, C. Cytoglobin Promotes Cardiac Progenitor Cell Survival against Oxidative Stress via the Upregulation of the NFκB/INOS Signal Pathway and Nitric Oxide Production. *Sci. Rep.* **2017**, *7* (1), 10754.
11. Shaw, R. J.; Omar, M. M.; Rokadiya, S.; Kogera, F. A.; Lowe, D.; Hall, G. L.; Woolgar, J. A.; Homer, J.; Liloglou, T.; Field, J. K.; et al. Cytoglobin Is Upregulated by Tumour Hypoxia and Silenced by Promoter Hypermethylation in Head and Neck Cancer. *Br. J. Cancer* **2009**, *101* (1), 139–144.
12. Cancer Research UK. Head and neck cancers mortality statistics https://www.cancerresearchuk.org/health-professional/cancer-statistics/statistics-by-cancer-type/head-and-neck-cancers/mortality#heading-One (accessed Apr 9, 2020).
13. Curry, J. M.; Sprandio, J.; Cognetti, D.; Luginbuhl, A.; Bar-Ad, V.; Pribitkin, E.; Tuluc, M. Tumor Microenvironment in Head and Neck Squamous Cell Carcinoma. *Semin. Oncol.* **2014**, *41* (2),
14. Peltanova, B.; Raudenska, M.; Masarik, M. Effect of Tumor Microenvironment on Pathogenesis of the Head and Neck Squamous Cell Carcinoma: A Systematic Review. *Mol. Cancer* **2019**, *18* (63).
15. Arantes, L. M. R. B.; De Carvalho, A. C.; Melendez, M. E.; Carvalho, A. L.; Goloni-Bertollo, E. M. Methylation as a Biomarker for Head and Neck Cancer. *Oral Oncology*. Elsevier Ltd 2014, pp 587–592.

16. Nam, H. J.; Baek, S. H. Epigenetic Regulation of the Hypoxic Response. *Curr. Opin. Psychol.* **2019**, *7*, 1–8.
17. Alsahafi, E.; Begg, K.; Amelio, I.; Raulf, N.; Lucarelli, P.; Sauter, T.; Tavassoli, M. Clinical Update on Head and Neck Cancer: Molecular Biology and Ongoing Challenges. *Cell Death Dis.* **2019**, *10*, 540.
18. Azharuddin, M.; Roberg, K.; Dhara, A. K.; Jain, V.; Darcy, P.; Hinkula, J.; Slater, N. K. H.; Patra, H. K. Dissecting Multi Drug Resistance in Head and Neck Cancer Cells Using Multicellular Tumor Spheroids. *Sci. Rep.* **2019**, *9*, 20066.
19. Costa, E. C.; Moreira, A. F.; de Melo-Diogo, D.; Gaspar, V. M.; Carvalho, M. P.; Correia, I. J. 3D Tumor Spheroids: An Overview on the Tools and Techniques Used for Their Analysis. *Biotechnology Advances*. Elsevier Inc. December 1, 2016, pp 1427–1441.
20. Ghosh, S.; Rao, P. B.; Kumar, P. R.; Manam, S. Concurrent Chemoradiation with Weekly Cisplatin for the Treatment of Head and Neck Cancers: An Institutional Study on Acute Toxicity and Response to Treatment. *Asian Pac. J. Cancer Prev.* **2015**, *16* (16), 7331–7335.
21. Le, X.; Hanna, E. Y. Optimal Regimen of Cisplatin in Squamous Cell Carcinoma of Head and Neck yet to Be Determined. *Ann. Transl. Med.* **2018**, *6* (11), 229.
22. Robinson, A. M.; Rathore, R.; Redlich, N. J.; Adkins, D. R.; Vanarsdale, T.; Van Tine, B. A.; Michel, L. S. Cisplatin Exposure Causes C-Myc-Dependent Resistance to CDK4/6 Inhibition in HPV-Negative Head and Neck Squamous Cell Carcinoma.
23. Widia Jusman, S. A.; Hambar Sari, D.; Suciati Ningsih, S.; Silvia Hardiany, N.; Sadikin, M. Role of Hypoxia Inducible Factor-1 Alpha (HIF-1$\alpha$) in Cytoglobin Expression and Fibroblast Proliferation of Keloids. *Kobe J. Med. Sci* **2019**, *65* (1), 10–18.
24. Fordel, E.; Geuens, E.; Dewilde, S.; De Coen, W.; Moens, L. Hypoxia/Ischemia and the Regulation of Neuroglobin and Cytoglobin Expression. *Life* **2004**, *56*, 681–687.
25. Mathai, C.; Jourd'heuil, F. L.; Lopez-Soler, R. I.; Jourd'heuil, D. Emerging Perspectives on Cytoglobin, beyond NO Dioxygenase and Peroxidase. *Redox Biol.* **2020**, *32*, 101468.
26. Kochanek, S. J.; Close, D. A.; Johnston, P. A. High Content Screening Characterization of Head and Neck Squamous Cell Carcinoma Multicellular Tumor Spheroid Cultures Generated in 384-Well Ultra-Low Attachment Plates to Screen for Better Cancer Drug Leads. *ASSAY Drug Development Technol.* **2019**, *17* (1), 17–36.
27. Hagemann, J.; Jacobi, C.; Hahn, M.; Schmid, V.; Welz, C.; Schwenk-Zieger, S.; Stauber, R.; Baumeister, P.; Becker, S. Spheroid-Based 3D Cell Cultures Enable Personalized Therapy Testing and Drug Discovery in Head and Neck Cancer. *Anticancer Res.* **2017**, *37* (5), 2201–2210.
28. Kadletz, L.; Heiduschka, G.; Domayer, J.; Schmid, R.; Enzenhofer, E.; Thurnher, D. Evaluation of Spheroid Head and Neck Squamous Cell Carcinoma Cell Models in Comparison to Monolayer Cultures. *Oncol. Lett.* **2015**, *10* (3), 1281–1286.
29. Braunholz, D.; Saki, M.; Niehr, F.; Öztürk, M.; Puértolas, B. B.; Konschak, R.; Budach, V.; Tinhofer, I. Spheroid Culture of Head and Neck Cancer Cells Reveals an Important Role of EGFR Signalling in Anchorage Independent Survival. *PLoS One* **2016**.
30. Kwon Byeon, H.; Ku, M.; Yang, J. Beyond EGFR Inhibition: Multilateral Combat Strategies to Stop the Progression of Head and Neck Cancer. *Exp. Mol. Med.* **2019**, *51* (8).
31. Stone, L. C.; Thorne, L. S.; Weston, C. J.; Graham, M.; Hodges, N. J. Cytoglobin Expression in the Hepatic Stellate Cell Line HSC-T6 Is Regulated by Extracellular Matrix Proteins Dependent on FAK-Signalling. *Fibrogenesis Tissue Repair* **2011**, *8* (1), 15.
32. Sato-Matsubara, M.; Matsubara, T.; Daikoku, A.; Okina, Y.; Longato, L.; Rombouts, K.; Thi Thanh Thuy, L.; Adachi, J.; Tomonaga, T.; Ikeda, K.; et al. Fibroblast Growth Factor 2 (FGF2) Regulates Cytoglobin Expression and Activation of Human Hepatic Stellate Cells via JNK Signaling. *J. Biol. Chem.* **2017**, *292* (46), 18961–18972.
33. Riss, T.; Niles, A.; Moravec, R.; Karassina, N.; Vidugiriene, J. *Cytotoxicity Assays: In Vitro Methods to Measure Dead Cells*; Eli Lilly & Company and the National Center for Advancing Translational Sciences, 2004.
34. Mosmann, T. Rapid Colorimetric Assay for Cellular Growth and Survival: Application to Proliferation and Cytotoxicity Assays. *J. Immunol. Methods* **1983**, *65* (1–2), 55–63.
35. Livak, K. J.; Schmittgen, T. D. Analysis of Relative Gene Expression Data Using Real-Time Quantitative PCR and the 2(-Delta Delta C(T)) Method. *Methods* **2001**, *25*, 402–408.
36. Zhou, Y.; Zhou, B.; Pache, L.; Chang, M.; Khodabakhshi, A. H.; Tanaseichuk, O.; Benner, C.; Chanda, S. K. Metascape Provides a Biologist-Oriented Resource for the Analysis of Systems-Level Datasets. *Nat. Commun.* **2019**, *10*, 1523.
37. Tyanova, S.; Cox, J. Perseus: A Bioinformatics Platform for Integrative Analysis of Proteomics Data in Cancer Research. In *Cancer Systems Biology: Methods and Protocols*; von Stechow, L., Ed.; Springer New York: New York, NY, 2018; pp 133–148.
38. Thorne, L. S.; Rochford, G.; Williams, T. D.; Southam, A. D.; Rodriguez-Blanco, G.; Dunn, W. B. and Hodges, N. J.; Cytoglobin protects cancer cells from apoptosis by regulation of mitochondrial cardiolipin. Scientific Reports. **2021**; Article number 985
39. Gang, G.-T.; Kim, Y.-H.; Noh, J.-R.; Kim, K.-S.; Jung, J.-Y.; Shong, M.; Hwang, J. H.; Lee, C.-H. Protective Role of NAD(P)H:Quinone Oxidoreductase 1 (NQO1) in Cisplatin-Induced Nephrotoxicity. *Toxicol. Lett.* **2013**, *221* (3), 165–175.
40. Xinarianos, G.; McRonald, F. E.; Risk, J. M.; Bowers, N. L.; Nikolaidis, G.; Field, J. K.; Liloglou, T. Frequent Genetic and Epigenetic Abnormalities Contribute to the Deregulation of Cytoglobin in Non-Small Cell Lung Cancer. *Hum. Mol. Genet.* **2006**, *15* (13), 2038–2044.
41. Beckerson, P.; Svistunenko, D.; Reeder, B. Effect of the Distal Histidine on the Peroxidatic Activity of Monomeric Cytoglobin. *F1000Research* **2015**, *4* (87).
42. Reeder, B. J.; Ukeri, J. Strong Modulation of Nitrite Reductase Activity of Cytoglobin by Disulfide Bond Oxidation: Implications for Nitric Oxide Homeostasis. *Nitric Oxide* **2018**, *72*, 16–23.
43. Singh, S.; Manda, S. M.; Sikder, D.; Birrer, M. J.; Rothermel, B. A.; Garry, D. J.; Mammen, P. P. A. Calcineurin Activates Cytoglobin Transcription in Hypoxic Myocytes. *J. Biol. Chem.* **2009**, *284* (16), 10409–10421.

44. Vinci, M.; Gowan, S.; Boxall, F.; Patterson, L.; Zimmermann, M.; Court, W.; Lomas, C.; Mendiola, M.; Hardisson, D.; Eccles, S. A. Advances in Establishment and Analysis of Three-Dimensional Tumor Spheroid-Based Functional Assays for Target Validation and Drug Evaluation. *BMC Biol.* **2012**, *10*, 29.
45. Nunes, A. S.; Barros, A. S.; Costa, E. C.; Moreira, A. F.; Correia, I. J. 3D Tumor Spheroids as in Vitro Models to Mimic in Vivo Human Solid Tumors Resistance to Therapeutic Drugs. *Biotechnol. Bioeng.* **2019**, *116* (1), 206–226.
46. Singh, S.; Wu, S.-Y.; Canseco, D. C.; Manda, S. M.; Nguyen, T.; Ye, Q. Cytoglobin Regulates Proliferation and Differentiation by Homeostatic and Stress Induced Repression of P53 Transcriptional Activity | Circulation. In *Genetics, Genomics and Congenital CV Disorders*; 2018; p A20541.
47. Singh, S.; Canseco, D.; Grinsfelder, D.; Bock-Marquette, Ii. Cytoglobin: A Novel Epicardial Regulator of Epithelial to Mesenchymal Transition (EMT) Within the Ischemic Heart | Circulation. In *Fibroblast Modulation in Cardiac Remodeling*; 2018; p A11639.
48. Bischin, C.; Taciuc, V.; Silaghi-Dumitrescu, R.; Cisplatin effect on hemoglobin and myoglobin autoxidation. *Studia UBB Chemia, LV*. **2010**, 4, 313-318.
49. Rowland, L. K.; Campbell, P. S.; Mavingire, N.; Wooten, J. V.; McLean, L.; Zylstra, D.; Thorne, G.; Daly, D.; Boyle, K.; Whang, S.; et al. Putative Tumor Suppressor Cytoglobin Promotes Aryl Hydrocarbon Receptor Ligand-Mediated Triple Negative Breast Cancer Cell Death. *J. Cell. Biochem.* **2019**, *120* (4), 6004–6014.
50. Liu, J.; Jiang, G.; Mao, P.; Zhang, J.; Zhang, L.; Liu, L.; Wang, J.; Owusu, L.; Ren, B.; Tang, Y.; et al. Down-Regulation of GADD45A Enhances Chemosensitivity in Melanoma. *Sci. RePORTS* | **2018**, *8*, 4111.
51. Duensing, S.; Swilling, N. W.; Hasskarl, J.; Hinds, P. W.; Mü Nger, K. Abrogation of the Retinoblastoma Tumor Suppressor Checkpoint During Keratinocyte Immortalization Is Not Sufficient for Induction of Centrosome-Mediated Genomic Instability. *Cancer Res.* **2003**, *63*, 476–483.
52. Jin, X.; Beck, S.; Sohn, Y. W.; Kim, J. K.; Kim, S. H.; Yin, J.; Pian, X.; Kim, S. C.; Choi, Y. J.; Kim, H. Human Telomerase Catalytic Subunit (HTERT) Suppresses P53-Mediated Anti-Apoptotic Response via Induction of Basic Fibroblast Growth Factor. *Exp. Mol. Med.* **2010**, *42* (8), 574–582.
53. Riffle, S.; Pandey, R. N.; Albert, M.; Hegde, R. S. Linking Hypoxia, DNA Damage and Proliferation in Multicellular Tumor Spheroids. *BMC Cancer* **2017**, *17*, 338.
54. Abraham, A. G.; O'Neill, E. PI3K/Akt-Mediated Regulation of P53 in Cancer. In *Biochemical Society Transactions*; Portland Press Ltd, 2014; Vol. 42, pp 798–803.
55. Choudhry, H.; Harris, A. L. Advances in Hypoxia-Inducible Factor Biology. *Cell Metab.* **2018**, *27*, 281–298.
56. Shaw, R. J.; Liloglou, T.; Rogers, S. N.; Brown, J. S.; Vaughan, E. D.; Lowe, D.; Field, J. K.; Risk, J. M. Promoter Methylation of P16, RARb, E-Cadherin, Cyclin A1 and Cytoglobin in Oral Cancer: Quantitative Evaluation Using Pyrosequencing. *Br. J. Cancer* **2006**, *94*, 561–568.
57. Kim, Y.; Jin Nam, H.; Lee, J.; Young Park, D.; Kim, C.; Suk Yu, Y.; Kim, D.; Won Park, S.; Bhin, J.; Hwang, D.; et al. Methylation-Dependent Regulation of HIF-1a Stability Restricts Retinal and Tumour Angiogenesis. *Nat. Commun.* **2016**, *7*, 10347.
58. Ross, D.; Siegel, D. NQO1 in Protection against Oxidative Stress. *Current Opinion in Toxicology*. Elsevier B.V. February 1, 2018, pp 67–72.
59. Zhou, H.-Z.; Zeng, H.-Q.; Yuan, D.; Ren, J.-H.; Cheng, S.-T.; Yu, H.-B.; Ren, F.; Wang, Q.; Qin, Y.-P.; Huang, A.-L.; et al. NQO1 Potentiates Apoptosis Evasion and Upregulates XIAP via Inhibiting Proteasome-Mediated Degradation SIRT6 in Hepatocellular Carcinoma. *Cell Cummunication Signal.* **2019**, *17*, 168.
60. Oh, E.-T.; Kim, J.-W.; Kim, J. M.; Kim, S. J.; Lee, J.-S.; Hong, S.-S.; Goodwin, J.; Ruthenborg, R. J.; Jung, M. G.; Lee, H.-J.; et al. NQO1 Inhibits Proteasome-Mediated Degradation of HIF-1alpha. *Nat. Commun.* **2016**, *7*, 139–706.
61. Stadler, M.; Scherzer, M.; Walter, S.; Holzner, S.; Pudelko, K.; Riedl, A.; Unger, C.; Kramer, N.; Weil, B.; Neesen, J.; et al. Exclusion from Spheroid Formation Identifies Loss of Essential Cell-Cell Adhesion Molecules in Colon Cancer Cells. *Sci. Rep.* **2018**, *8*, 1151.
62. Schmidt, M.; Scholz, C. J.; Polednik, C.; Roller, J. Spheroid-Based 3-Dimensional Culture Models: Gene Expression and Functionality in Head and Neck Cancer. *Oncol. Rep.* **2016**, *35* (4), 2431–2440.
63. Haass, N. K.; Ripperger, D.; Wladykowski, E.; Dawson, P.; Gimotty, P. A.; Blome, C.; Fischer, F.; Schmage, P.; Moll, I.; Brandner, J. M. Melanoma Progression Exhibits a Significant Impact on Connexin Expression Patterns in the Epidermal Tumor Microenvironment. *Histochem. Cell Biol.* **2010**, *133* (1), 113–124.
64. Hanna, S.; El-Sibai, M. Signaling Networks of Rho GTPases in Cell Motility. *Cellular Signalling*. October 2013, pp 1955–1961.
65. Phuyal, S.; Farhan, H. Multifaceted Rho GTPase Signaling at the Endomembranes. *Front. Cell Dev. Biol.* **2019**, *7*, 127.
66. Zhan, T.; Rindtorff, N.; Boutros, M. Wnt Signaling in Cancer. *Oncogene* **2017**, *36*, 1461–1473.
67. Hong, C. F.; Chen, W. Y.; Wu, C. W. Upregulation of Wnt Signaling under Hypoxia Promotes Lung Cancer Progression. *Oncol. Rep.* **2017**, *38* (3), 1706–1714.
68. Xu, W.; Zhou, W.; Cheng, M.; Wang, J.; Liu, Z.; He, S.; Luo, X.; Huang, W.; Chen, T.; Yan, W.; et al. Hypoxia Activates Wnt/β-Catenin Signaling by Regulating the Expression of BCL9 in Human Hepatocellular Carcinoma. *Sci. Rep.* **2016**, *7*, 40445.